The phototrophic anaerobic model no 1 (PAM-1): a mechanistic model for anaerobic phototrophs in wastewater applications

D. PUYOL, E. BARRY, T. HUELSEN, KENN LU, J. KELLER, D. BATSTONE.

JOURNAL SELECTED: WATER RESEARCH

NUMBERING (without tables and figures): 7999 words

NUMBER OF TABLES: 3

NUMBER OF FIGURES: 6

ABSTRACT

TO BE COMPLETED AFTER PAPER CORRECTION.

Key words: Phototrophic bacteria, resource recovery, mechanistic modelling, Partition-Release-Recovery

1 INTRODUCTION

Wastewater treatment is shifting focus from not just treatment, but also capture and recovery of organics and nutrients. This requires novel technological approaches. A key approach is to utilise fast growing organisms to concentrate energy, nutrients, and trace compounds into the solid phase, and hence substantially reduce reactive removal of nitrogen and organics while enabling phosphorous recovery. One option is high-rate activated sludge, which can achieve 40% nitrogen removal in the primary stage through adsorption and assimilation (Jetten et al. 1997). Algae can also be used to partition, but simultaneous heterotrophic and photosynthetic mode is only possible in bacterial-algal associations that reduce organic substrate consumption efficiency (Muñoz and Guieysse 2006).. Purple phototrophic bacteria are a promising new partitioning approach, which have been shown to completely remove nitrogen to discharge limits when sufficient organic carbon is present without the need for pure cultures, and using IR light only as a driver for growth (Hulsen et al. 2014a).

PPB grow phototrophically rather than photosynthetically, and do not use water as an electron donor to produce oxygen and organics. They are among the most metabolically versatile organisms on earth (Hunter et al. 2008). They grow heterotrophically using a wide range of organic compounds, both in presence and absence of light (photoheterotrophy and chemoheterotrophy) (Hunter et al. 2008). But they can growth autotrophically as well by using infrared light as the energy driver for CO_2 fixation,

and different inorganic electron donors for the lithotrophic process, as H_2, Fe^{2+}, S^{2-} or $S_2O_3^{2-}$ (cyclic anoxygenic photosynthesis) (Overmann and Garcia-Pichel 1998). Though they can grow in the presence of oxygen, they are extremely effective in anaerobic photoheterotrophic conditions (McKinlay and Harwood 2010, Gordon and McKinlay 2014). Their ability to recycle electrons during the cyclic anoxygenic photosynthesis gives them a very high efficiency on electrons cycles. They can even accumulate electrons in form of reduced cofactors that they need to dispose for redox balancing. This can be done through two main strategies: (i) ATP-driven hydrogen production by ferredoxin oxidation in the hydrogenase/nitrogenase system at the end of the electron transport chain (ETC), and (ii) increasing the assimilative growth by re-fixation of CO_2 via Calvin Cycle produced during heterotrophic metabolism (McKinlay and Harwood 2010). These metabolic features give them the possibility of growing and over-competing other microorganisms in heterogeneous phototrophic environments that promote the microbial growth, as low-mid strength wastewater systems with low hydraulic retention times (HRT) (Hulsen et al. 2014b).

PPB present also other interesting features for their use in wastewater systems. They are able to accumulate polymers as poly-phosphate (poly-P) (Liang et al. 2010), polysaccharides (Klein et al. 1991), poly-β hidroxybutyrate (PHB) (Melnicki et al. 2009) and other poly-3(hydroxyalkanoates) (PHA) (Brandl et al. 1991). And, under an excess of organics and available energy, they can be the main actor in biogenic hydrogen systems (Basak and Das 2007).

PPB have been assessed for wastewater treatment, particularly for processing swine wastewater (Kim et al. 2004), latex rubber-sheet wastewater (Kantachote et al. 2005), tofu wastewater (Zhu et al. 1999), or sugar refinery wastewater (Yetis et al. 2000). However, most of these studies were focused more on hydrogen production rather than organics removal or nutrient recovery (Tao et al. 2008, Fang et al. 2005, Lee et al. 2010). They have also been applied on domestic wastewater (DWW) in batch and continuous operation to completely remove nitrogen to discharge limits when sufficient organic carbon is present without the need for pure cultures, and using IR light only as a driver for growth (Hulsen et al. 2014a). This enables complete treatment of wastewater in a single step at comparable hydraulic retention times and to a similar standard as activated sludge processes, without destruction of the nitrogen and phosphorous.

Modelling is ubiquitously used to design, benchmark, and analyse wastewater treatment systems, with the IWA Activate Sludge Model (ASM)-family models being probably the most well-known (Henze et al. 2006). The IWA anaerobic digestion model no. 1 (ADM-1) is the analogous model for domestic and industrial anaerobic systems (Batstone et al. 2002). The IWA Models, and wastewater modelling in general has generally applied first order hydrolysis for solids transformation (including decay),

Monod for uptake kinetics and inverse Monod (non-competive) for inhibition functions, and the use of COD for organics and molar for inorganic compounds. Obviously development of new technologies using novel vectors such as PPB requires development of a similar mechanistic model.

There are complex metabolic models based on PPB metabolism primarily focused on the electron transport chain (Golomysova et al. 2010, Klamt et al. 2002). Due to its complexity, this is motivated more on pure scientific development rather than a real field application. These models are not suitable for a wastewater model due to high amount of model components that cannot be measured in a routine fashion, therefore validation is not possible. There has also been work done on modelling PPB to describe hydrogen production only (Obeid et al. 2009, Eroglu 2008, Gadhamshetty et al. 2008), limited to this specific application (organics in excess with limited ammonium). But due to DWW composition, the key growth modes for DWW treatment are photoheterotrophy (principal) as well as chemoheterotrophy and photoautotrophy growth modes, depending on wastewater composition. Biochemical mechanisms relevant to complex substrates such as solids hydrolysis and biomass decay have to be addressed as well. Therefore, this work is aiming to propose a mechanistic model based on the utilization of PPB as partition agent in DWW treatment with general applicability to also industrial wastewater and the ability to interpret mixed culture metabolic processes.

2. Materials and Methods

2.1 Model Description

The model was developed to be units-compatible with the IWA ASM and ADM series (Henze et al. 2006, Batstone et al. 2002). Therefore, units are gCOD L^{-1} (or kgCOD m^{-3}) for both soluble and particulates as in the ADM1. Nutrient units are in gN L^{-1} and gP L^{-1}, respectively, with bicarbonate in gC L^{-1}.

Monod kinetics is generally applied for biological growth processes, with first order kinetics for hydrolysis and decay. Monod or non-competitive inhibition has been applied for limiting or inhibitory expressions respectively. Because of a lack of functional differentiation in the PPB biomass, and limited evidence to the contrary, only one biomass component has been selected (PPB). Other biological groups present in ASM and ADM1 models (e.g., hydrogen utilising methanogens) could be readily included. As in the ASM/ADM models S_i is used for soluble compounds, and X_i for particulate compounds, where subscript *i* denotes the compound.

The model does not currently include poly-P or other polymer accumulation, since this occurs mainly in static (not growing) mode (Liang et al. 2010, Hiraishi et al. 1991), and to limit model scope. Likewise nitrification/denitrification processes are not included, since they can only occur in aerobic conditions

where the NH_4^+ can be oxidized to nitrite or nitrate. Therefore, N and P are removed by assimilative growth only.

In presence of organic substrates, photoheterotrophy through the tri-carboxylic acid (TCA) cycle dominates. Two major mechanisms of electron disposal by PPB are considered. Production of CO_2 (S_{IC}) is a key feature of PPB biomass at growing conditions (McKinlay and Harwood 2010) and is important for closing the C balance. The oxidation state of the organic compound determines if the biomass needs CO_2 for substrate uptake (reduced substrates like propionate, butyrate or valerate), or the uptake produces CO_2 (oxidized substrates like acetate, succinate or ethanol)(McKinlay and Harwood 2011). In this later case, the biomass disposes the excess of electrons in growing conditions by re-fixing the CO_2 produced in the TCA cycle. As a consequence the total balance of CO_2 in the system remains close to neutrality. A theoretical explanation of this mechanism is explained in Supplementary Information. The other major mechanism of electron disposing by PPB is the H_2 production via Nitrogenase complex. In static mode, the PPB biomass is able to use the excess of electrons for redox balance at the end of the ETC. The ferredoxin complex is the carrier for this process, but the biomass need energy in form of ATP (Golomysova et al. 2010). However, this process has been claimed to be inhibited in presence of NH_4^+, a strong inhibitor of the nitrogenase activity (Rodionov et al. 1986). Indeed, this process has been studied and demonstrated that H_2 production is inhibited In a DWW fed situation due to (i) presence of ammonium and (ii) disposing of electrons by CO_2 re-fixation that promotes the growth (see Supplementary Information for more details). Therefore, it can be deduced that CO_2 production and re-fixation into de Calvin Cycle is the major electron sink in the PPB metabolism treating DWW. In absence of organic substrates, the biomass performs completely autotrophic growth using reduced inorganic compounds other than water for growing (anoxygenic photosynthesis). Sulfur cycle is out of the model due to low sulfate concentration in DWW and model simplification. It is however possible to add sulfate reduction into the model with subsequent sulphide utilisation as an electron donor for autotrophic PPB growth, which would require to add another biomass component (PPB cannot perform sulfate reduction). PPB can perform chemoheterotrophy at a lower rate, providing H_2 (S_{h2}) to the photoautotrophy mechanism (Golomysova et al. 2010).

Transforming these mechanisms to a practical enables the following key processes (Figure 1):-

(i) Photoheterotrophic metabolism on acetate (S_{ac}) (acetate uptake). This involves acetate assimilation by PPB when light is present. Acetate was separated by the other substrates due to differentiation observed due to batch tests. Due to an imbalance in substrate-biomass carbon oxidation state, this process results in production also of CO_2.

(ii) Photoheterotrophic metabolism on other organics (S_S) (photoheterotrophic uptake). These include all soluble organics that PPB can assimilate to growth in light conditions, including non-acetate VFAs, alcohols, and some sugars. These have been lumped into a single soluble substrate. Likewise for (i) this results in uptake of CO_2.

(iii) Chemoheterotrophic metabolism (chemoheterotrophic uptake). This mechanism involves the assimilative consumption of any organic in dark conditions that can be metabolized through either fermentation or anaerobic oxidation processes. All these processes have been joined as one mechanism for a shake of simplicity. This process involves H_2 and acetate as end products. Acetate is not further oxidised through chemoheterotrophy due to a lack or very limited terminal electron acceptors such as Fe(III) and sulfate (Finneran et al. 2003).

(iv) Photoautotrophic metabolism (autotrophic uptake). This mechanism involves the assimilative CO_2 fixation by PPB in light conditions using H_2 as the electron donor for the process. Other electron donors have been omitted but could be easily added to the model components, as Fe^{2+}, S^{2-} and $S_2O_3^-$.

(v) PPB cell decay (decay). This mechanism involves the deactivation of PPB by cell death. Ammonium, phosphate and inorganic carbon are released during this process and the biomass is converted into composites.

(vi) Hydrolysis and particulate fermentation (hydrolysis). The decomposition of particulates into organics (S_{ac} and S_S), ammonium, phosphate, hydrogen and inorganic carbon is addressed as a sole mechanism for simplicity. Both soluble and particulate inerts are also products of this process. A breakdown of particulate fermentation can be incorporate into the model according to the ADM-1 in particular cases (especially for long SRT processes).

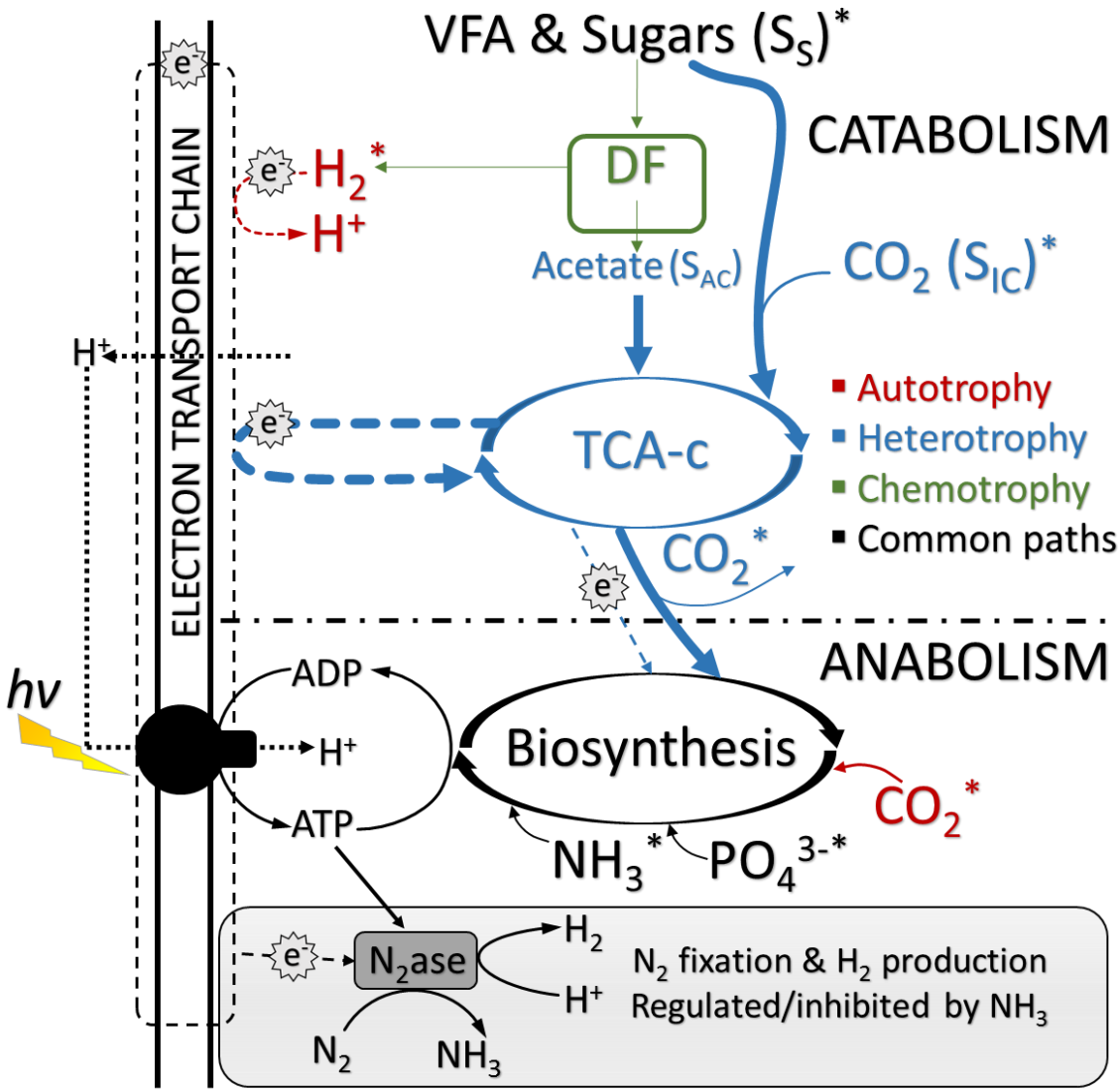

150

151 **Figure 1:** Schematic summary of PPB metabolism under domestic wastewater treatment. Key: N2ase:
152 Nitrogenase complex. TCA-c: Tri-carboxylic acid cycle. DF: Dark fermentation. VFA: volatile fatty acids.
153 e^-: electrons. Dash: electron cycles. Dot: proton pumps. *: Model compounds.

154 The model is presented as Petersen matrix notation in Table 2. A complete set of

155 Kinetic parameters were generally obtained from the batch experiments, or from the literature as
156 described below. Saturation constant for hydrogen consumption by photoautotrophic process ($K_{S,h2}$)
157 light limitation ($K_{S,E}$) and inhibition by ammonia ($K_{I,FA}$) were set arbitrarily low. Stoichiometry is based
158 on theoretical calculations from literature, as well as verified experimentally.. The model is balanced
159 in COD, C, N and P. HCO_3^-, NH_4^+ and PO_4^{2-} have been used for closing C, N and P balances, respectively.

Table 2. Petersen matrix of the PAM-1 model for domestic wastewater treatment by PPB.

Component (C) → i		1	2	3	4	5	6	7	8	9	10
j	Process↓	S_S	S_{ac}	S_{IC}	S_{h2}	S_{IN}	S_{IP}	S_I	X_{PB}	X_C	X_I
1	Hydrolysis/fermentation	$f_{ss,xc}$	$f_{Sac,xc}$	$f_{IC,XC}$	$f_{h2,XC}$	$f_{IN,xc}$	$f_{IP,xc}$	$f_{si,xc}$	0	-1	$f_{xi,xc}$
2	Acetate uptake	0	-1	$f_{IC,ph,ac}$	0	$-f_{N,B}Y_{PB,ph}$	$-f_{P,B}Y_{PB,ph}$	0	$Y_{PB,ph}$	0	0
3	Photoheterotrophic uptake	-1	0	$-f_{IC,ph,Ss}$	0	$-f_{N,B}Y_{PB,ph}$	$-f_{P,B}Y_{PB,ph}$	0	$Y_{PB,ph}$	0	0
4	Chemoheterotrophic uptake	-1	$(1-Y_{PB,ch})f_{ac,ch}$	0	$(1-Y_{PB,ch})f_{h2,ch}$	$-f_{N,B}Y_{PB,ch}$	$-f_{P,B}Y_{PB,ch}$	0	$Y_{PB,ch}$	0	0
5	Autotrophic uptake	0	0	$-f_{IC,a}$	$-f_{h2,a}$	$-f_{N,B}Y_{PB,a}$	$-f_{P,B}Y_{PB,a}$	0	$Y_{PB,a}$	0	0
6	Decay of XPB	0	0	$-\sum_{i=8-9} Ci \times f_{C,i}$	0	$-\sum_{i=8-9} Ci \times f_{N,i}$	$-\sum_{i=8-9} Ci \times f_{P,i}$	0	-1	1	0
		Soluble substrate (g COD L^{-1})	Acetate (g COD L^{-1})	Inorganic carbon (mg C_HCO_3 L^{-1})	H_2 (g COD L^{-1})	Inorganic nitrogen (g N_NH_4 L^{-1})	Inorganic phosphorous (g P_PO_4 L^{-1})	Soluble inert (g COD L^{-1})	Phototrophic biomass (g COD L^{-1})	Composite biomass (g COD L^{-1})	Particulate inert (g COD L^{-1})

Supplementary information contains description of model components, full kinetic parameters and stoichiometric coefficients (S1), determination and calibration of stoichiometry (S2), and a full list of model equations (S4).

The model was implemented in Aquasim 2.1d and Matlab and is available on request from the corresponding author. Parameters were obtained from batch experiments (including Monod parameters) through non-linear parameter estimation as previously described (Batstone et al. 2003) by minimisation of residual sum of squares (J=RSS), with parameter uncertainty determined using two-tailed *t*-test calculated from standard error in parameter value. Where parameter optimisation problems involve multiple parameters (k_m, K_S), parameter uncertainty surface ($J=J_{crit}$) has also been assessed as described in(Batstone et al. 2003) .

2.2 Batch Experiments

A number of batch experiments were done to identify parameters based on the model description. Detailed experimental methods are provided in supplementary information, but briefly described here. The inoculum was from a lab-scale continuous photo-anaerobic membrane bioreactor (PAnMBR) described by (Hulsen et al. 2015 REF-Continuous paper-) operated over 300d. Domestic wastewater was collected from the Taringa wastewater lift station (Brisbane, Australia) with an average strength of 572 mgCOD L^{-1} and soluble COD of 241 mgCOD L^{-1}, 63 mgN L^{-1}, and 9 mgP L^{-1}.

Where wastewater was not the medium, synthetic Ormerod media was used at pH 7.5 as described previously (Hulsen et al. 2014a).

Metabolic growth batch tests. All batch tests were done in 100mL working volume (160 mL serum flasks) in triplicate, inoculated from the PAnMBR reactor. Headspace was flushed with N_2 and experiments carried out at 20°C in an orbital shatter set at 150 rpm (Edwards Instrument Company. Lighting was by 150W lamps using UV-VIS absorbing foil as described elsewhere (Hulsen et al. 2014a). All experiments were accompanied by no-substrate blank tests, where required, by positive and negative controls. A summary is provided in Table 1

Table 1: Batch conditions of the different metabolic tests.

Mechanism	Medium	Buffer system*	COD/N/P (C/N/P)***	C source (mgCOD L^{-1})	Electron donor (mg L^{-1})	Electron acceptor	Positive control	Negative control
Photoheterotrophy	Ormerod	HEPES	100/10/2	Acetate (130), propionate, butyrate, ethanol (100)	Organic	CO2	Adding 1 g $NaHCO_3$	-

Nitrogen limitation	Ormerod	HEPES	100/1.4/2	Acetate (130)	Organic	CO2	No N limitation	-
Phosphorus limitation	Ormerod	HEPES	100/10/0.15	Acetate (130)	Organic	CO2	No P limitation	-
Photoautotrophy	Ormerod	Phosphate	(100/20/∞)	NaHCO3 (140)**	Na_2S (300)	CO2	-	No Na_2S
Chemoheterotrophy (dark)	Ormerod	HEPES	100/10/2	Ethanol (60), Acetate (130)	Organic	Acetate	With light	-
Inhibition of H_2 production	DWW	-	100/12/4	DWW (278)	Organic	CO2	-	Acetate (600)
	Ormerod	Phosphate	100/15/∞	Acetate (600)	Organic	CO2	-	N limitation (1/10)

* Buffer systems: HEPES (5.9 g L^{-1}), Phosphate (0.9 g K_2HPO_4 + 0.66 g KH_2PO_4). ** mg C L^{-1} *** ∞ means in high excess due to buffering

Hydrolysis and biomass decay Inoculum (0.5 L) was collected as above (2.1 g VSS L^{-1}). The biomass was centrifuged in 50 mL Falcon tubes and the pellet resuspended again in NaCl 0.2 M three times. Biomass was then placed in 0.5 L of NaCl 0.2 M and was divided into two 0.25 L Schott bottles, which were subsequently flushed with N_2 and magnetically stirred at 200 rpm. The bottles were operated for 30 d.

One of the bottles was covered with aluminium foil to avoid phototrophic activity, and was used for the hydrolysis analysis. Liquid sampling was performed twice a week to analyse volatile fatty acids (VFAs), NH_4-N, PO_4-P, total inorganic carbon (TIC) and pH. Headspace was analysed for CH_4, H_2 and CO_2. TSS/VSS, TKN and TP was analysed every 7 d.

The other bottle was illuminated as indicated above without feed, and biomass samples were taken every 7 d to assess activity (determining decay coefficient). Activity tests were done as above with 100 mgCOD L^{-1} of acetate and 10 mg NH_4-N L^{-1}.

Calculation of Specific Phototrophic Activities (SPA). Model based analysis is generally used to determine parameters as described above, but specific phototrophic activity was also determined by linear regression of substrate concentration over a minimum of four points through the region of maximum consumption divided by biomass concentration.

2.3 Analytical methods

TCOD and SCOD were determined by COD cell tests (Merck, 1.14541.0001, Darmstadt, Germany). Dissolved NH_4 -N, NO_2-N and PO_4-P were determined by a QuikChem8000 Flow Injection Analyzer (FIA) (Hach Company, Loveland, USA). Temperature and pH were measured using an Oakton pH 11 Series (Vernon Hill, IL, USA). TSS and VSS were determined by filtration according to standard methods, where TSS were calculated after drying the sample in an oven at 105 ± 2 °C and VSS were calculated after burning it in a furnace at 550 ± 5 °C (APHA. 1998). Illuminance (W m^{-2}) was measured with an IR

light sensor (PAS Port™, Roseville, CA, USA). VFA samples were analysed by gas chromatography (Agilent Technologies 7890A GC System, Santa Clara, CA, USA) equipped with a flame ionisation detector (GC/FID) and a polar capillary column (DB-FFAP). Gas samples were analysed by GC (2014 Shimadzu, Kyoto, Japan) with thermal coupled detector (TCD) (Tait et al. 2009). TKN and TP were determined using sulfuric acid, potassium sulfate and copper sulfate catalyst in a block digestor (Lachat BD-46, Hach Company, Loveland, CO, USA) (Patton and Truitt 1992). TIC was analysed by using a total organic carbon (TOC) analyser (Shimadzu TOC-L CSH TOC Analyser with TNM-L TN unit) coupled to a near infrared detector (NIRD) for measuring the CO_2. All soluble constituents were determined after filtering with a 0.45 µm membrane filter (Millipore, Millex®-HP, Merck Group, Darmstadt, Germany).

1.1.1 Data handling

Biomass concentration was calculated in g VSS L^{-1}, and it was further transformed into COD by using the COD relationship calculated from the biomass equation $CH_{1.8}O_{0.38}N_{0.18}$ (McKinlay and Harwood 2010) (1 g biomass expressed as VSS = 1.78 g COD).

Biomass yields (*Y*) were calculated accounting for the initial and final biomass concentration (in g VSS L^{-1}) based on substrate consumption. Biomass concentration was further transformed into COD and then yields are expressed as g $COD_{biomass}$ g^{-1} COD.

Statistical analyses

All the parameters were calculated from triplicate batch/measurements. Confidence intervals (at 95%) were also calculated and used for statistical representative comparisons.

3. Results

The sludge used for all the experiments that came from the lab-scale PAnMBR (Hülsen et al 2015 REF CONTINUOUS PAPER) Most of the microorganisms are related with α-*proteobacteria,* where PPB clearly dominates accounting for more than 70% of the total gene copies detected by the pyrosequencing technique. The genus *Rhodobacter* ssp. is the most represented in the microbiota with more than 60%. The presence of other phototrophs as microalgae and cyanobacteria is residual, with less than 1% of total gene copies. Therefore, the biomass can be considered as PPB-dominant biomass, which all the light processes being carried out by PPB exclusively.

3.1 Growth Processes

Photoheterotrophy were assessed with VFA and ethanol as substrate (Fig 2a). All the substrates were completely consumed in the experimental time, and the growing efficiency was in all cases similar, with an average biomass yield was calculated to be 1.13 ± 0.21 g $COD_{biomass}$ g^{-1} COD. As can be seen in

Figure 2b, non-acetate substrates were similar, with a k_m of 1.3±0.1 (gCOD.gCOD^{-1}d^{-1}), and undetectable K_S (not different from 0.0 gCOD L^{-1}), while acetate had a significantly higher k_m (2.4±0.2 gCOD.gCOD^{-1}d^{-1}) and higher (though still very low) K_S of 0.02±0.01 gCOD L^{-1}. Essentially this means that growth (uptake) is faster on acetate, but that with a lower affinity such that acetate uptake is faster at the beginning of the batch, but slower at the end.

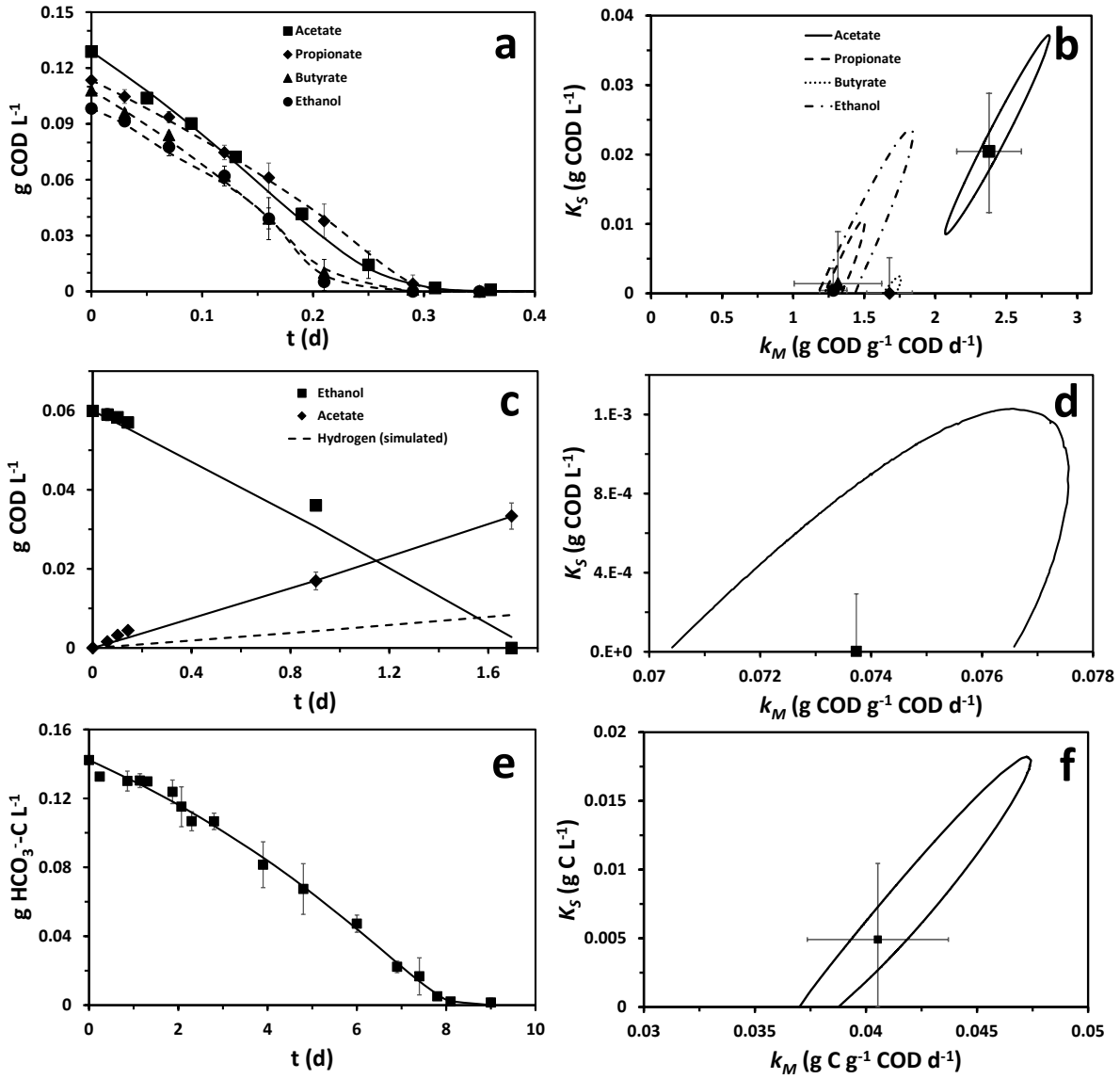

Figure 2: Experimental (symbols) and modelled (lines) time curse of substrates uptake (left) and parameters determination including 95% confidence intervals and confidence regions (right) of PPB metabolism in photoheterotrophy (a), chemoheterotrophy (b) and photoautotrophy (c) growth modes.

Analysis of the chemoheterotrophic metabolism by PPB was conducted by using acetate and ethanol as substrates in dark conditions (Figure 2c). PPB biomass was much less effective in dark conditions rather than in light conditions (biomass yield 0.5 vs 1.1 g $COD_{biomass}$ g^{-1} COD in dark and light conditions, respectively). Also the Monod parameters, calculated by using the stoichiometry of the anaerobic syntrophic ethanol oxidation to acetate (Seitz et al. 1990), are approximately half that of photoheterotrophy (Figure 2d), though with again, extremely low K_S values. While chemotrophic growth is not dominant under photoheterotrophic conditions, it can be very important to consider in reactor design (e.g., where there is insufficient light). COD, C and nutrient balances.

Analysis of photoautotrophy was done with $NaHCO_3$ as C source and Na_2S as electron donor in 5-fold stoichiometric excess (see Table 1) (Figure 2e). The biomass had a yield of 3.0 g $COD_{biomass}$ g^{-1} IC comparable to the value on acetate (2.63g $COD_{biomass}$ g^{-1} C). However, maximum uptake rate was far slower at 0.04±0.005 gC gCOD d^{-1} (compared to 0.9±0.2 gC gCOD d^{-1} on acetate) Figure 2f. Photoautotrophy needs to be considered both to close balances, and in the case where there is an excess of bicarbonate and electrons (but not organics) in wastewater.

Nutrient limitation experiments for N and P were used to determine saturation coefficients for N and P and K_S values were extremely low such that the N and P regulation became a switch function (data shown in SI). Biomass assimilated nutrients at a COD/N/P ratio of 100/7.1/1.8, which is higher than conventional aerobic bacteria and much higher than other anaerobes (Tchobanoglous et al. 2003). These values are in line with previous works (Hulsen et al. 2014a). However, PPB were able to grow at a lower rate once the nutrients were completely consumed (42% lower than in full nutrients conditions), likely due to fixation of headspace N_2 (Hunter et al. 2008) (inhibited in the presence of ammonium). Also, PPB can accumulate polymers like poly-phosphate (Liang et al. 2010) as well as PHA (Melnicki et al. 2009), which can be used in static mode for growing. Since the model developed here promotes biomass growth (growing mode) with presence of ammonium, nutrient limitation for growing have to be included.

3.2 Endogenous processes – hydrolysis and decay.

Hydrolysis and decay are considered as transversal first order biochemical processes in most models (Henze et al. 2006, Szilveszter et al. 2010, Batstone et al. 2006). These could be considered separately, since phototrophic activity can be considered separately by withdrawal of illumination (noting that decay occurred in illumination without substrate), thus replicating reactor conditions. Figure 3 shows the time course of the SPA values (on acetate) calculated for the PPB biomass suffering the starvation. The biomass reduced in activity according to a first order model with decay coefficient of 0.09 ± 0.02 d^{-1}. Hydrolysis was done in dark conditions, to avoid reassimilation of products by PPB, considering

that hydrolysis enzymes are currently present. Hydrolysis also followed a first order model with a decay coefficient of 0.071 ± 0.004 d^{-1} (Fig 4). It should be noted that hydrolysis is substrate specific, and is highly situation specific (Batstone et al. 2015), but that a value of 0.1 d^{-1} is comparable with hydrolysis kinetics under anaerobic conditions.

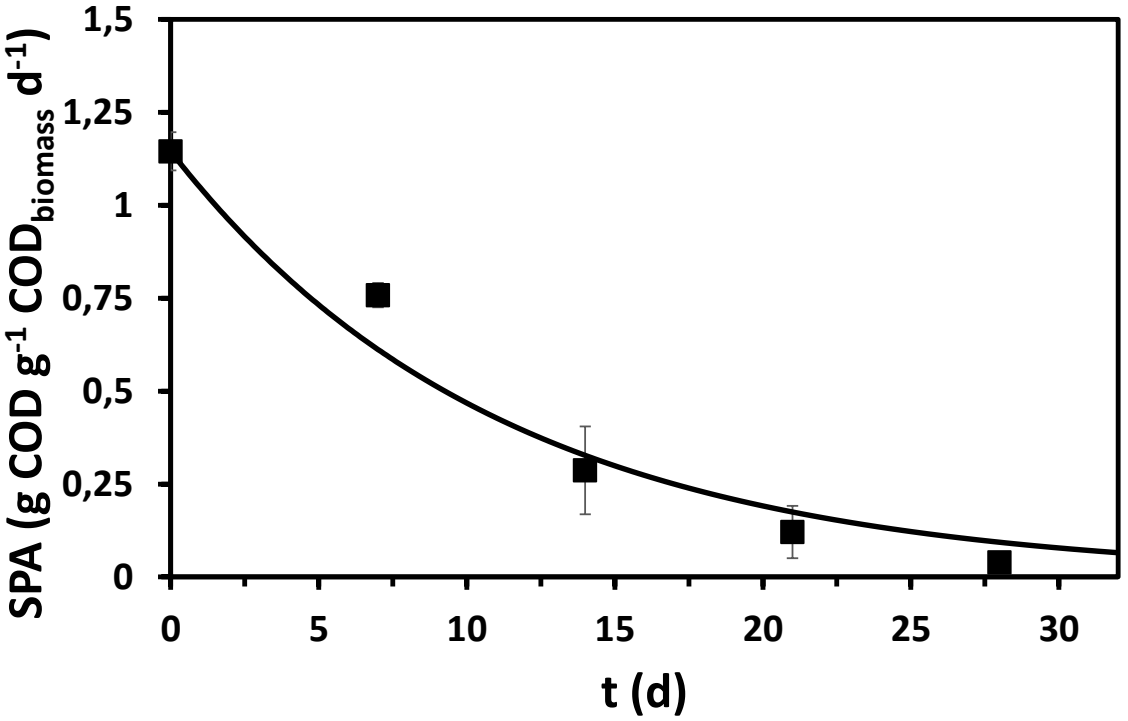

Figure 3: Mechanism of decay rate. Time course of specific phototrophic activity of PPB subjected to starvation under full illumination.

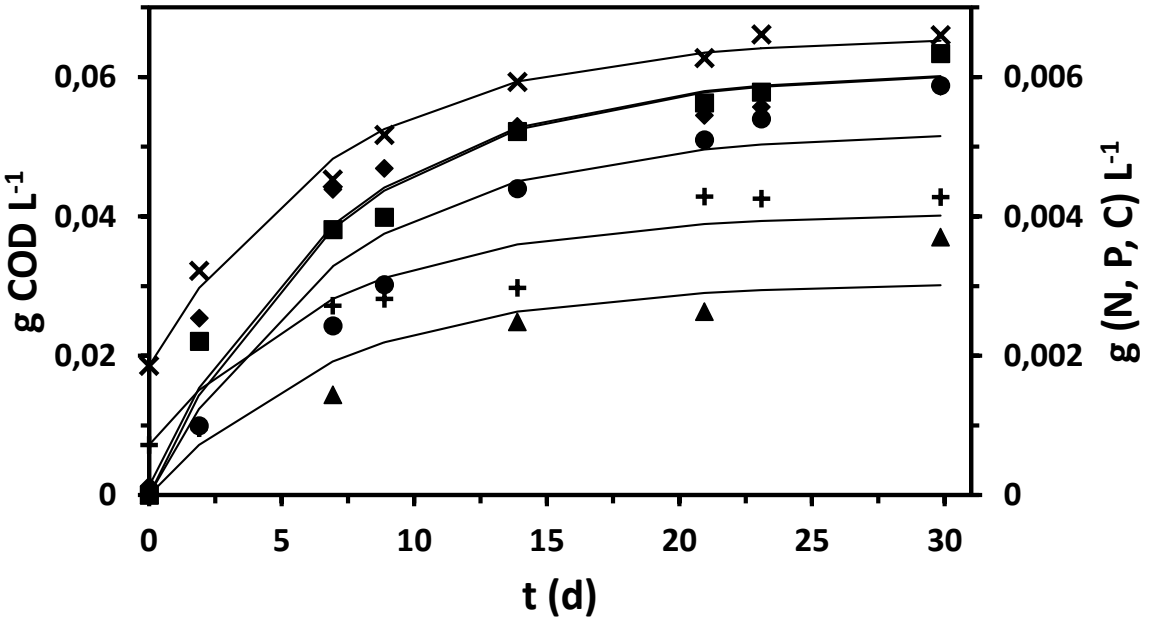

Figure 4: Mechanism of hydrolysis. Time course of released products upon starvation in dark conditions: soluble organic compounds but acetate (squares), acetate (diamonds), hydrogen (triangles), TIC (pluses), NH_4^+-N (circles) and PO_4^{3-}-P (crosses).

4. Discussion

4.1 Parameter values vs pure culture PPB

A full list of parameter values can be found in Supplementary Material, whereas Table 3 shows parameters determined from the literature in comparison with those reported here. Parameters were calculated on the basis that (i) protein composition of PPB is in all cases 60% of dry weight(McKinlay and Harwood 2010), (ii) 1 g VSS = 1.78 g COD and (iii) PPB biomass equation is $CH_{1.8}O_{0.38}N_{0.18}$(McKinlay and Harwood 2010).

In general, biomass yields calculated here are well in line with values reported in the literature (Table 3). The only exception is the biomass yield for autotrophic growth. Values are difficult to access and only indirect calculation can be performed. (Wang et al. 1993) reported biomass growth and CO_2 fixation in *Rhodobacter sphaeroides* and *Rhodospirillum rubrum* using different electron sources (H_2, thiosulfate, sulphide and malate) and the biomass yield values extracted from their activities considerably vary with an average value of 7 g COD g^{-1} C fixed, which strongly differs from the value reported here (3.0 ± 0.2 g COD g^{-1} C fixed) that is very close to the theoretical maximum yield for carbon dioxide fixation of (3.32 g COD g^{-1} C). Re-fixation of CO_2 coming from malate may considerably underestimate real CO_2 usage for growing in the Calvin cycle (McKinlay and Harwood 2011).

However, specific uptake rates were substantially different to the literature values, which may be due to pure culturing in contrast with mixed cultures used in the present work. For chemoheterotrophic parameters, an example is found in (Schultz and Weaver 1982) where the growth rates of *Rhodospirillum rubrum* and *Rhodopseudomonas capsulata* were studied on several chemoheterotrophic substrates in the dark. The authors used trimethylamine-N-oxide as accessory electron acceptor activity on fructose, glucose and succinate. Photoheterotrophic parameters also diverged. However, while acetate uptake rates are similar to the values reported here (Golomysova et al. 2010, McKinlay and Harwood 2011), those obtained from other organics, as malate (Klein et al. 1991, Gadhamshetty et al. 2008), lactate+malate (Obeid et al. 2009), or butyrate (McKinlay and Harwood 2011) were much higher, which have been obtained in hydrogen production studies. Under these situations, the substrate uptake is optimized for biogenic H_2 by dislocating catabolism from anabolism, considerably increasing the substrate uptake rate while minimising yield (Basak and Das 2007). Therefore specific growth rates (μ_{max}, d^{-1}) and doubling times (d) are more indicated for establishing comparisons. The μ_{max} for photoheterotrophic metabolism was calculated to be 1.54 d^{-1}, which corresponds to 0.45 d of doubling time. It is similar to those reported by (McKinlay and Harwood 2011) (0.27-0.44 d), and generally aligns well with purple phototrophic bacteria (Hunter et al. 2008). Pure culturing (the most of parameters reported in Table 3) promotes specific uptake rates in decrement of substrate affinity, which lets to increased k_M and K_S parameters, a typical behaviour of r-strategist microorganisms (Dorodnikov et al. 2009).

Hydrolysis and decay rates are very dependent on the material at hand, and the system redox conditions. In general, for a given material hydrolysis coefficient increases from anaerobic to anoxic, and from anoxic to aerobic (Henze et al. 2006). The biomass decay and hydrolysis constants found in the literature were obtained in aerobic photoheterotrophic processes (Huang et al. 1999, Huang et al. 2001), which explains that they are considerably higher than those calculated here.

Compared with previous analysis, this study is focused on mixed culture photoheterotrophic metabolism. The biomass seems to be a K-strategist which promoting substrate affinity over uptake, a microbial strategy in low-strength systems as domestic wastewater with low hydraulic retention times (less than 12 h), which is useful for over-competing other fast-growing microorganisms, and clearly effective vs the slow growing methanogens, which are the only competitors for acetate under anaerobic conditions with low sulfate or reduced metals concentration (Dorodnikov et al. 2009).

Table 3: Comparison of estimated parameters with those reported in the literature.

	$k_{M,ac}$	$k_{M,ph}$	$k_{M,ch}$	$k_{M,ic}$	$K_{S,s}$	$Y_{PB,ph}$	$Y_{PB,ch}$	$Y_{PB,a}$	k_{hyd}	k_{dec}

	$g\ COD\ g^{-1}\ COD\ d^{-1}$	$g\ COD\ g^{-1}\ COD\ d^{-1}$	$g\ COD\ g^{-1}\ COD\ d^{-1}$	$g\ IC\ g^{-1}\ COD\ d^{-1}$	$mg\ COD\ L^{-1}$	$g\ COD\ g^{-1}\ COD$	$g\ COD\ g^{-1}\ COD$	$g\ COD\ g^{-1}\ C$	d^{-1}	d^{-1}
Estimated	2.4	1.4	0.074	0.041	0.524	1.1	0.5	3	0.07	0.09
Literature average	1.5	11	5	0.3	4333	0.78	0.23	11	0.27	0.20
Standard deviation	0.5	13	4	0.2	6036	0.37	0.12	7	0.06	0.02
n (observations)	2	12	8	9	2	17	8	4	2	2
References	[1]	[2]	[3]	[4]	[5]	[6]	[7]	[8]	[9]	[10]

[1] (Golomysova et al. 2010, McKinlay and Harwood 2011), [2] (Klein et al. 1991, Golomysova et al. 2010, Obeid et al. 2009, Gadhamshetty et al. 2008, McKinlay and Harwood 2011), [3] (Schultz and Weaver 1982, Madigan and Gest 1978), [4] (Wang et al. 1993, Sarles and Tabita 1983), [5] (Obeid et al. 2009, Gadhamshetty et al. 2008), [6] (Klein et al. 1991, Klamt et al. 2002, Obeid et al. 2009, Gadhamshetty et al. 2008, McKinlay and Harwood 2011, Schultz and Weaver 1982), [7] (Schultz and Weaver 1982, Madigan and Gest 1978), [8] (Wang et al. 1993), [9] (Huang et al. 1999, Huang et al. 2001), [10] (Huang et al. 1999, Huang et al. 2001)

2 4.2 Model application

The model has been tested for exploring different scenarios and then knowing limits of the process as well as possible adaptations of the model by biomass shifts on metabolism. The model has been implemented in Matlab R2014a, where the simulations have been performed. Detailed information about the simulations is provided in Supplementary Information.

2.1 Scenario 1. Domestic wastewater with deficiency of C or nutrients (N and P)

In this scenario the main metabolic pathway to be analysed is the photoheterotrophic metabolism. Since the main outcome of the PRR concept is the complete assimilation of C, N and P by PPB, it is necessary to explore the limits of the process in terms of optimum COD/N/P conditions for typical DWW treatment systems.

Systematic (not-random) simulations have been performed with the main fixed components: biomass concentration (0.05 g COD L^{-1}), no light limitation and experimental time (2.5 d). More details are found in Supplementary Information. Variable conditions were soluble substrate (0.01-0.5 g COD L^{-1}), acetate (0.01 – 0.5 g COD L^{-1}), ammonium (0.005-0.065 g N L^{-1}) and phosphate (0.001-0.015 g P L^{-1}). A total of 2 sets of 50x50 simulations were performed by varying (i) SCOD and ammonium, and (ii) SCOD and phosphate. Figure 4 shows the results of the simulations. X-axis represents the initial

concentration of the sum of all soluble substrates, whereas Y-axis are the initial NH_4^+-N and PO_4^{2-}P concentration for Figures 4a and 4b, respectively. Values in the graphs represents normalized uptake efficiencies where 1.0 represents 100% removal of both soluble substrate and the respective nutrient. Values lower than 1.0 represent that one of the varying components is not fully consumed.

Optimum COD/N/P relationship has been calculated to be 100/7.1/1.8. According to Figure 4, there is three possible regions outside the optimum in a real case: (i) low nutrients concentration where there is a net accumulation of the SCOD in the system –overload- (ii) high nutrients concentration where all the SCOD is consumed but the effluents still contains N and P –underload-, and (iii) very low COD that is never going to be enough for maintaining biomass growth despite nutrients concentration. Region (iii) is the only that cannot be sustained in a long-term process due to biomass decay. Region (i) is not possible in a DWW scenario where nutrients are always in excess. It could be the case for other kind of wastewaters. Respect to the region (ii), that is the most typical case, it is clear that the only way of obtaining full nutrient removal is by adding external SCOD to the system. Figure 4 could serve as a quick guide for estimating the need for treatment in a real case.

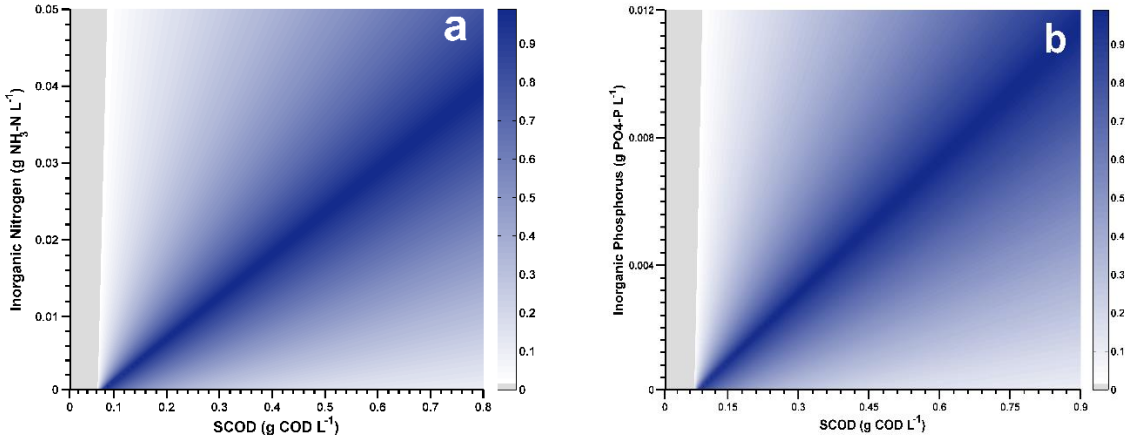

Figure 4. Normalized efficiency of SCOD and NH_4^+-N (a) or PO_4^{2-}-P (b) removal by PPB in a simulated scenario at different SCOD/N/P ratios, where maximum efficiency (1.0, dark blue) corresponds to total consumption of SCOD and nutrients. Grey area represents negative efficiencies, where the biomass decay is higher than growth and therefore is not sustainable.

2.2 Scenario 2. Effect of chemoheterotrophic processes in light-limiting conditions during light/dark cycles.

Parameters calculated in this work are conditioned by the origin of the biomass. The PAnMBR reactor was operated at full illumination with no light/dark cycles. Although this is the normal operation procedure for PPB, in some cases artificial illumination could be avoided by using natural sun light as energy source as happen usually with algae reactors (Christenson and Sims 2011). During dark (night)

cycles, the biomass need to make use of an energy source other than light so it is predictable that the metabolism would shift into mixed photo-chemoheterotrophy. Indeed, several authors have published that PPB are able to follow chemoheterotrophic metabolism achieving substrate uptakes rates at least one order of magnitude above the values calculated here (see Table 3). Therefore, it is necessary to explore how the system behaves under a promoted chemoheterotrophy during light/dark cycles.

A set of two simulations were performed by including light/dark cycles (1 h each for a total of 6 cycles) during a typical batch test scenario where all the conditions were fixed but the uptake rate for chemoheterotrophic metabolism was modified using two different values ($k_{M,ch}$ = 0.074 and 0.7 g COD g^{-1} COD d^{-1}). Conditions and rationality for the simulation are described in Supplementary Information. Results from the simulation are depicted in Figure 5. As can be seen, when the biomass have a high chemoheterotrophic activity, soluble substrate is consumed giving rise to acetate accumulation that is eventually consumed during light cycles. A net production of hydrogen happen due to fermentation/anaerobic oxidation processes, which can be used for promoting autotrophic growth. This can be also connotations on the possible biomass shift to autotrophic metabolism, as will be discussed later. Since the biomass yield is lower during chemoheterotrophic metabolism, there is a lower net increase of biomass.

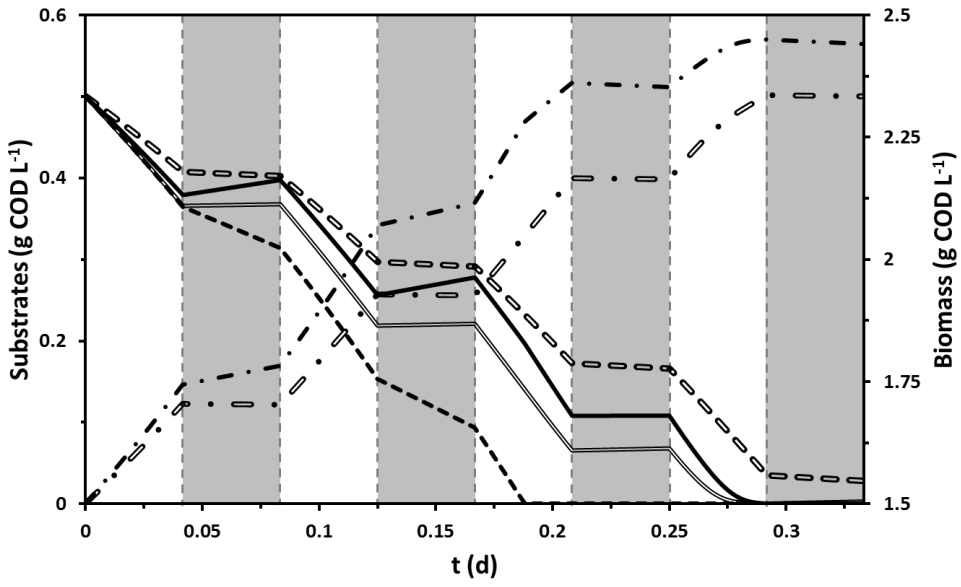

Figure 5. Effect of dark/light cycles on PPB metabolism under low (double lines) and high (single lines) chemoheterotrophic activity ($k_{M,ch}$ = 0.074 and 0.7 g COD g^{-1} COD d^{-1}, respectively). Simulation of the time course of acetate (continuous line), ethanol (dash line) and biomass (dash-dot lines) concentrations during 1 h dark/light periods.

2.3 Scenario 3. Promotion of carbon dioxide fixation in DWW coming from hard waters.

In this scenario the promotion of autotrophy is discussed and the autotrophic metabolism is analysed. The DWW used for the batch experiments and for the continuous PAnMBR came from a DWW collector located in Brisbane (Australia). Water in this place can be considered as moderately hard (hardness = 148 ± 7 mg $CaCO_3$ L^{-1}, n=19, which corresponds to 53 mg C L^{-1}). Therefore, there is a clear potential to enrich the PPB process in autotrophic conditions. However, this is only possible if there is an electron donor for the process, mainly Fe^{2+}, S^{2-} or H_2(Hunter et al. 2008), or reduced organics(McKinlay and Harwood 2011). The promotion of reductive processes as fermentation or anaerobic oxidation (including sulfate reduction as well) could give risen to the reduced components for carbon dioxide fixation to be feasible. This analysis is focused on the results after the reduced conditions appeared, so the discussion on how these conditions are possible is out of scope.

A simulation has been conducted to analyse how the model behaves on a promoted autotrophic metabolism scenario. To that purpose, the initial conditions have been fixed and only the H_2 concentration has been increased to 0.175 g COD L^{-1} to cope with the stoichiometric requirements of autotrophic carbon dioxide fixation. Then, the simulation has been performed by using the autotrophic uptake rate value calculated here ($k_{M,ic}$=0.041 g C g^{-1} COD d^{-1}) and a Gaussian-random set of 500 Montecarlo simulations using the average and 95% confidence intervals for the $k_{M,au}$ values reported in the literature (as reported in Table 3). Simulation conditions and rationality are described in Supplementary Material. The results are depicted in Figure 6. As can be seen, the autotrophic process using the calculated values seems to be residual compared to the photoheterotrophic metabolism. However, the autotrophic promotion can modify substantially the scenario. In the most probable case (using the mean of the $k_{M,ic}$ from Table 3), the biomass is able to fix 1 g TIC L^{-1} in the same time than they assimilate 1.76 g C L^{-1} by the photoheterotrophic metabolism. Therefore, the carbon dioxide fixation could become a major process, which potentially could account for around 36% of N and P removal.

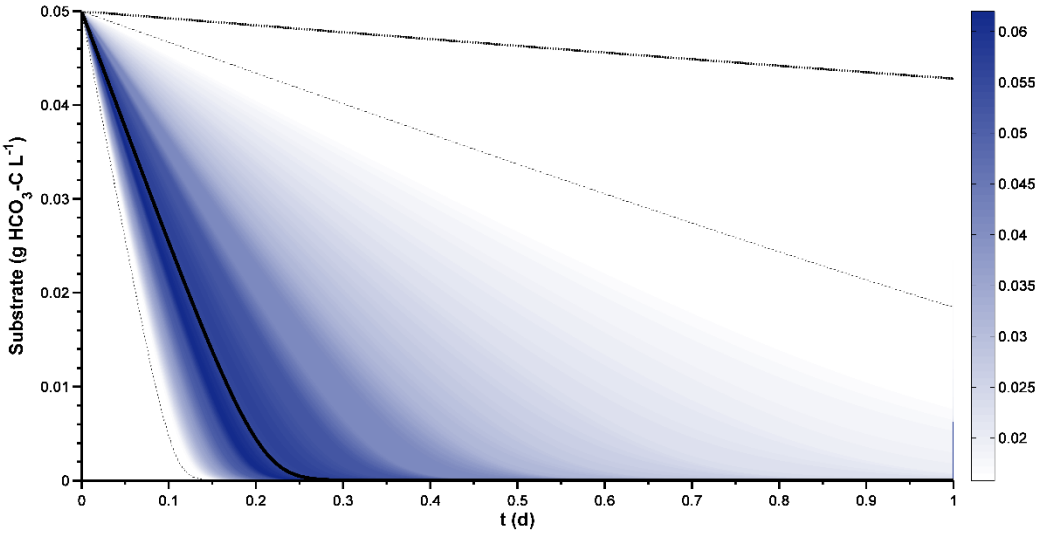

446

447 **Figure 6**. Photoautotrophic-promoted metabolism behaviour. Time course of inorganic carbon for $k_{M,IC}$
448 values obtained by a Gaussian-random set of Montecarlo simulations based on literature reported
449 values for phototrophic bacteria (blue shades), including the simulation using the mean (continuous
450 line) and 95% confidence intervals of the mean (short dot-points). It is also shown the simulation using
451 the parameter value determined in the present paper (dot line).

452 3 Recommendations, limitations and future work.

453 This study presents the first model for domestic wastewater treatment by purple phototrophic
454 bacteria, under the scope of the new platform proposed for domestic wastewater treatment, the
455 Partition-Release-Recovery concept, developed by (Batstone et al. 2014), and funded by the CRC for
456 Water Sensitive Cities Program and the Smart Water Fund. The model will serve as a basis for the
457 implementation of the technology in DWW treatment in Australia, as a first step, and then to spread
458 the technology overseas.

459 The model has described the following implications that can be used as recommendations for up-
460 scaling:

461 (i) The PPB process in DWW fed situation performs mainly through photoheterotrophic
462 metabolism. Maximum uptake rate is between 1.4-2.4 g COD g^{-1} COD d^{-1} with a biomass
463 yield of around 1 g COD g^{-1} COD. For a typical wastewater treatment plant, with a solid
464 retention time of 2 d and a TCOD of 1 g L^{-1}, it involves a minimum HRT of 5.7 h.
465 (ii) It is necessary to provide extra addition of SCOD to the system to cope with full nutrient
466 removal. The extra addition will depends on the wastewater composition, according to
467 the COD/N/P ratio of 100/7.1/1.8.

(iii) The chemoheterotrophic behaviour of the PPB biomass is very dependent on the DWW composition. It is recommended to study in detail this process in each particular case, especially in systems designed with light/dark cycles.

The model has the following limitations:

(i) This model is for domestic wastewater treatment only. It is not recommended to use for any other kind of wastewater without the necessary modifications.

(ii) The model is only valid for anaerobic conditions, and hydrogen production for redox balancing is assumed to be inhibited, so this model cannot be implemented for hydrogen production systems as it is.

(iii) The model is not contemplating poly-P as well as other polymers accumulation. Also, nitrogen fixation is not included since it is assumed to be inhibited by ammonium.

(iv) This model represents a simplification of PPB metabolism, and includes biological mechanisms only. Implementation in full case needs to include hydrodynamics, light harvesting, gas phase addition, ionic charges and pH simulation. An update of the model is currently ongoing and will be implemented in a real Pilot-plant set-up.

Future work will includes the upgrading of the model to cope with the limitations. Specifically, we are currently addressing poly-P and PHA accumulation as well as N_2 fixation and side H_2 production. The effect of specific components/characteristics of wastewater other than domestic are also been addressing (as typical heavy metals –Cu and Zn-, low and high pH and their combined effect with ammonium and free ammonia, and components of specific wastewaters as pharmacs, hormones, aromatic volatiles or biocides, among others).

4 ACKNOWLEDGEMENTS

This work was jointly funded by the Smart Water Fund (project 10OS-023) and the CRC for Water Sensitive Cities (project C2.1). Thanks are given to Prof. James B. McKinlay for his kind discussion on PPB metabolism.

5 REFERENCES

Jetten, M.S.M., Horn, S.J. and van Loosdrecht, M.C.M. (1997) Towards a more sustainable municipal wastewater treatment system. Water Science and Technology 35(9), 171-180.

Muñoz, R. and Guieysse, B. (2006) Algal–bacterial processes for the treatment of hazardous contaminants: A review. Water research 40(15), 2799-2815.

Hulsen, T., Batstone, D.J. and Keller, J. (2014a) Phototrophic bacteria for nutrient recovery from domestic wastewater. Water research 50, 18-26.

Hunter, C.N., Daldal, F., Thurnauer, M.C. and Beatty, J.T. (2008) The Purple Phototrophic Bacteria, Springer.
Overmann, J. and Garcia-Pichel, F. (1998) The phototrophic way of life: The Prokaryotes: an evolving electronic resource for the microbiological community. M. Dworkin, New York, Springer.
McKinlay, J.B. and Harwood, C.S. (2010) Carbon dioxide fixation as a central redox cofactor recycling mechanism in bacteria. Proceedings of the National Academy of Sciences of the United States of America 107(26), 11669-11675.
Gordon, G.C. and McKinlay, J.B. (2014) Calvin cycle mutants of photoheterotrophic purple nonsulfur bacteria fail to grow due to an electron imbalance rather than toxic metabolite accumulation. J Bacteriol 196(6), 1231-1237.
Hulsen, T., Batstone, D.J. and Keller, J. (2014b) Phototrophic bacteria for nutrient recovery from domestic wastewater. Water Res 50, 18-26.
Liang, C.-M., Hung, C.-H., Hsu, S.-C. and Yeh, I.-C. (2010) Purple nonsulfur bacteria diversity in activated sludge and its potential phosphorus-accumulating ability under different cultivation conditions. Applied Microbiology and Biotechnology 86(2), 709-719.
Klein, G., Klipp, W., Jahn, A., Steinborn, B. and Oelze, J. (1991) The relationship of biomass, polysaccharide and H2 formation in the wild-type and nifA/nifB mutants of Rhodobacter capsulatus. Archives of Microbiology 155(5), 477-482.
Melnicki, M.R., Eroglu, E. and Melis, A. (2009) Changes in hydrogen production and polymer accumulation upon sulfur-deprivation in purple photosynthetic bacteria. International Journal of Hydrogen Energy 34(15), 6157-6170.
Brandl, H., Gross, R.A., Lenz, R.W., Lloyd, R. and Fuller, R.C. (1991) The accumulation of poly(3-hydroxyalkanoates) in Rhodobacter sphaeroides. Archives of Microbiology 155(4), 337-340.
Basak, N. and Das, D. (2007) The prospect of purple non-sulfur (PNS) photosynthetic bacteria for hydrogen production: the present state of the art. World Journal of Microbiology and Biotechnology 23(1), 31-42.
Kim, M.K., Choi, K.-M., Yin, C.-R., Lee, K.-Y., Im, W.-T., Lim, J.H. and Lee, S.-T. (2004) Odorous swine wastewater treatment by purple non-sulfur bacteria, Rhodopseudomonas palustris, isolated from eutrophicated ponds. Biotechnology letters 26(10), 819-822.
Kantachote, D., Torpee, S. and Umsakul, K. (2005) The potential use of anoxygenic phototrophic bacteria for treating latex rubber sheet wastewater. Electronic Journal of Biotechnology 8(3), 314-323.
Zhu, H., Suzuki, T., Tsygankov, A.A., Asada, Y. and Miyake, J. (1999) Hydrogen production from tofu wastewater by Rhodobacter sphaeroides immobilized in agar gels. International Journal of Hydrogen Energy 24(4), 305-310.
Yetis, M., Gündüz, U., Eroglu, I., Yücel, M. and Türker, L. (2000) Photoproduction of hydrogen from sugar refinery wastewater by Rhodobacter sphaeroides OU 001. International Journal of Hydrogen Energy 25(11), 1035-1041.
Tao, Y., He, Y., Wu, Y., Liu, F., Li, X., Zong, W. and Zhou, Z. (2008) Characteristics of a new photosynthetic bacterial strain for hydrogen production and its application in wastewater treatment. International Journal of Hydrogen Energy 33(3), 963-973.
Fang, H.H.P., Liu, H. and Zhang, T. (2005) Phototrophic hydrogen production from acetate and butyrate in wastewater. International Journal of Hydrogen Energy 30(7), 785-793.
Lee, H.-S., Vermaas, W.F. and Rittmann, B.E. (2010) Biological hydrogen production: prospects and challenges. Trends Biotechnol 28(5), 262-271.
Henze, M., Gujer, W., Mino, T. and Van Loosedrecht, M. (2006) Activated sludge models ASM1, ASM2, ASM2d and ASM3.
Batstone, D.J., Keller, J., Angelidaki, I., Kalyuzhnyi, S., Pavlostathis, S., Rozzi, A., Sanders, W., Siegrist, H. and Vavilin, V. (2002) The IWA Anaerobic Digestion Model No 1(ADM 1). Water Science & Technology 45(10), 65-73.

Golomysova, A., Gomelsky, M. and Ivanov, P.S. (2010) Flux balance analysis of photoheterotrophic growth of purple nonsulfur bacteria relevant to biohydrogen production. International Journal of Hydrogen Energy 35(23), 12751-12760.
Klamt, S., Schuster, S. and Gilles, E.D. (2002) Calculability analysis in underdetermined metabolic networks illustrated by a model of the central metabolism in purple nonsulfur bacteria. Biotechnol Bioeng 77(7), 734-751.
Obeid, J., Magnin, J., Flaus, J., Adrot, O., Willison, J. and Zlatev, R. (2009) Modelling of hydrogen production in batch cultures of the photosynthetic bacterium Rhodobacter capsulatus. International Journal of Hydrogen Energy 34(1), 180-185.
Eroglu, I. (2008) Hydrogen production by Rhodobacter sphaeroides O.U.001 in a flat plate solar bioreactor. International Journal of Hydrogen Energy 33(2), 531-541.
Gadhamshetty, V., Sukumaran, A., Nirmalakhandan, N. and Theinmyint, M. (2008) Photofermentation of malate for biohydrogen production— A modeling approach. International Journal of Hydrogen Energy 33(9), 2138-2146.
Hiraishi, A., Yanase, A. and Kitamura, H. (1991) Polyphosphate Accumulation by Rhodobacter sphaeroides Grown under Different Environmental Conditions with Special Emphasis on the Effect of External Phosphate Concentrations. Bulletin of Japanese Society of Microbial Ecology 6(1), 25-32.
McKinlay, J.B. and Harwood, C.S. (2011) Calvin cycle flux, pathway constraints, and substrate oxidation state together determine the H2 biofuel yield in photoheterotrophic bacteria. MBio 2(2), e00323-00310.
Rodionov, Y.V., Lebedeva, N.V. and Kondratieva, E.N. (1986) Ammonia inhibition of nitrogenase activity in purple and green bacteria. Archives of Microbiology 143(4), 345-347.
Finneran, K.T., Johnsen, C.V. and Lovley, D.R. (2003) Rhodoferax ferrireducens sp. nov., a psychrotolerant, facultatively anaerobic bacterium that oxidizes acetate with the reduction of Fe(III). International Journal of Systematic and Evolutionary Microbiology 53(3), 669-673.
Batstone, D.J., Pind, P.F. and Angelidaki, I. (2003) Kinetics of thermophilic, anaerobic oxidation of straight and branched chain butyrate and valerate. Biotechnol Bioeng 84(2), 195-204.
APHA. (1998) Standard Methods for the Examination of Water and Wastewater. 20th ed. American Public Health Association, Washington, DC, USA.
Tait, S., Tamis, J., Edgerton, B. and Batstone, D.J. (2009) Anaerobic digestion of spent bedding from deep litter piggery housing. Bioresource technology 100(7), 2210-2218.
Patton, C.J. and Truitt, E.P. (1992) Methods of Analysis by the US Geological Survey National Water Quality Laboratory: Determination of the Total Phosphorus by a Kjeldahl Digestion Method and an Automated Colorimetric Finish that Includes Dialysis, US Geological Survey.
Seitz, H.J., Schink, B., Pfennig, N. and Conrad, R. (1990) Energetics of syntrophic ethanol oxidation in defined chemostat cocultures - 1. Energy requirement for H2 production and H2 oxidation. Archives of Microbiology 155(1), 82-88.
Tchobanoglous, G., Burton, F.L., Stensel, H.D., Metcalf and Eddy (2003) Wastewater Engineering: Treatment and Reuse, McGraw-Hill Education.
Szilveszter, S., Ráduly, B., Ábrahám, B., Lányi, S. and Niculae, D.R. (2010) Mathematical models for domestic biological wastewater treatment process. Environmental Engineering and Management Journal 9(5), 629-636.
Batstone, D.J., Keller, J. and Steyer, J. (2006) A review of ADM 1 extensions, applications, and analysis: 2002-2005. Water Science and Technology 54(4), 1-10.
Batstone, D.J., Puyol, D., Flores-Alsina, X. and Rodríguez, J. (2015) Mathematical modelling of anaerobic digestion processes: applications and future needs. Reviews in Environmental Science and Bio/Technology 14(4), 595-613.
Wang, X., Modak, H.V. and Tabita, F.R. (1993) Photolithoautotrophic growth and control of CO2 fixation in Rhodobacter sphaeroides and Rhodospirillum rubrum in the absence of ribulose bisphosphate carboxylase-oxygenase. J Bacteriol 175(21), 7109-7114.

601 Schultz, J. and Weaver, P. (1982) Fermentation and anaerobic respiration by Rhodospirillum rubrum
602 and Rhodopseudomonas capsulata. J Bacteriol 149(1), 181-190.
603 Dorodnikov, M., Blagodatskaya, E., Blagodatsky, S., Fangmeier, A. and Kuzyakov, Y. (2009)
604 Stimulation of r- vs. K-selected microorganisms by elevated atmospheric CO2 depends on soil
605 aggregate size: Research article. FEMS Microbiology Ecology 69(1), 43-52.
606 Huang, J.S., Jih, C.G. and Sung, T.J. (1999) Performance enhancement of suspended-growth reactors
607 with phototrophs. Journal of Environmental Engineering 125(6), 501-507.
608 Huang, J.S., Wu, C.S., Jih, C.G. and Chen, C.T. (2001) Effect of addition of Rhodobacter sp. to
609 activated-sludge reactors treating piggery wastewater. Water Res 35(16), 3867-3875.
610 Madigan, M.T. and Gest, H. (1978) Growth of a photosynthetic bacterium anaerobically in darkness,
611 supported by “oxidant-dependent” sugar fermentation. Archives of Microbiology 117(2), 119-122.
612 Sarles, L.S. and Tabita, F.R. (1983) Derepression of the synthesis of D-ribulose 1, 5-bisphosphate
613 carboxylase/oxygenase from Rhodospirillum rubrum. J Bacteriol 153(1), 458-464.
614 Christenson, L. and Sims, R. (2011) Production and harvesting of microalgae for wastewater
615 treatment, biofuels, and bioproducts. Biotechnology Advances 29(6), 686-702.
616 Batstone, D.J., Hülsen, T., Mehta, C.M. and Keller, J. (2014) Platforms for energy and nutrient
617 recovery from domestic wastewater: A review. Chemosphere (0).

618